

Generic Contrast Agents

Our portfolio is growing to serve you better. Now you have a *choice*.



FRESENIUS
KABI

[VIEW CATALOG](#)

AJNR

T1-weighted three-dimensional magnetization transfer MR of the brain: improved lesion contrast enhancement.

D A Finelli, G C Hurst and R P Gullapalli

AJNR Am J Neuroradiol 1998, 19 (1) 59-64

<http://www.ajnr.org/content/19/1/59>

This information is current as
of May 28, 2025.

T1-Weighted Three-dimensional Magnetization Transfer MR of the Brain: Improved Lesion Contrast Enhancement

Daniel A. Finelli, Greg C. Hurst, and Rao P. Gullapalli

PURPOSE: We developed and evaluated clinically T1-weighted three-dimensional gradient-echo magnetization transfer (MT) sequences for contrast-enhanced MR imaging of the brain.

METHODS: A short-repetition-time, radio frequency–spoiled, 3-D sequence was developed with a 10-millisecond MT pulse at high MT power and narrow MT pulse-frequency offset, and the enhancing lesion-to-normal white matter background (L/B) and the contrast-to-noise (C/N) ratios on these images were compared with those on T1-weighted spin-echo images and on non-MT 3-D gradient-echo images in a prospective study of 45 patients with 62 enhancing lesions. In the 24 patients who had intracranial metastatic disease, the number of lesions was counted and compared on the three types of images.

RESULTS: The MT ratio of normal callosal white matter was 55% on the MT 3-D gradient-echo sequences. The L/B and C/N on the MT 3-D gradient-echo images were more than double those on the 3-D gradient-echo images, and were significantly greater than those on the T1-weighted spin-echo images. In patients with metastatic disease, the MT 3-D gradient-echo images showed significantly more lesions than did the T1-weighted spin-echo or 3-D gradient-echo images.

CONCLUSION: MT 3-D gradient-echo MR imaging improves the contrast between enhancing lesion and background white matter over that obtained with conventional T1-weighted 3-D gradient-echo and spin-echo imaging. MT 3-D gradient-echo imaging provides practical sampling, image coverage, and spatial resolution, attributes that may be advantageous over MT T1-weighted spin-echo techniques.

Several studies have shown an improvement in the contrast between enhancing lesions and normal white matter background (L/B) on contrast-enhanced T1-weighted magnetic resonance (MR) images obtained with the magnetization transfer (MT) technique (1–10). A practical limitation to the use of T1-weighted spin-echo imaging with MT has been the prolongation of the minimum repetition time (TR) per section, which reduces the section coverage for short-TR spin-echo images. Prolongation of the minimum TR per section can also result in decreased effective MT power (root mean squared B_1 amplitude) if one has

reached the limits of the MT pulse peak amplitude that can be delivered by the radio-frequency (RF) amplifier (11–13).

Lesion contrast on three-dimensional gradient-echo contrast-enhanced images was initially reported to be comparable to that on T1-weighted spin-echo images (14, 15). Subsequently, the 3-D gradient-echo images were shown, in general, to have poorer contrast than the T1-weighted spin-echo images, and the notion became established that small mildly enhancing lesions without edema, such as small metastatic lesions or multiple sclerosis plaques, may be missed on 3-D gradient-echo images (16, 17). Recently, it has been shown that when comparably thick sections are used, with comparable signal-to-noise (S/N) ratio (obtained by averaging several adjacent 3-D gradient-echo thin sections to the width of a corresponding 5- to 8-mm spin-echo section), the L/B and contrast-to-noise (C/N) ratios may actually be greater on 3-D gradient-echo sequences than on T1-weighted spin-echo images (18, 19). We sought to improve the detectability of small enhancing lesions further by combining the high-resolution and large image cov-

Received December 20, 1996; accepted after revision May 8, 1997.

From the Department of Radiology, MetroHealth Medical Center, Case Western Reserve University School of Medicine, Cleveland, Ohio (D.A.F.); IMIG-MRI Systems, I.I.c., Acton, Mass (G.C.H.); and the Department of Radiology, University of Maryland Medical Center, College Park (R.P.G.).

Address reprint requests to Daniel A. Finelli, MD, Department of Radiology, MetroHealth Medical Center, 2500 MetroHealth Dr, Cleveland, OH 44109.

erage attributes of short-echo-time (TE)/short-TR RF-spoiled T1-weighted 3-D gradient-echo images with the augmented L/B of contrast-enhanced T1-weighted spin-echo sequences obtained with MT. A T1-weighted MT 3-D gradient-echo sequence was developed, and the L/B and C/N ratios on these images were compared with those on T1-weighted spin-echo and non-MT 3-D gradient-echo images in a prospective study of 45 patients with 62 enhancing lesions.

Methods

Forty-five patients referred for contrast-enhanced MR examinations were studied between January 1995 and June 1996. The patients were selected because of known enhancing primary brain tumors or known cerebral metastatic disease, which had been documented on previous MR or computed tomographic (CT) studies. Examinations were performed on a 1.5-T imager, using a circularly polarized head coil. The research was conducted with approval of the institutional review board, and informed consent was obtained from the patients. Diagnoses included primary brain tumor ($n = 10$), meningioma ($n = 6$), acoustic schwannoma ($n = 5$), and cerebral metastases from lung or breast carcinoma ($n = 24$).

Sequence Techniques

The axial T1-weighted 3-D RF-spoiled gradient-echo sequence was performed with the following parameters: 25/4.4/1 (TR/TE/excitations), a 22° flip angle, 24 5-mm-thick sections, a 25-cm field of view (FOV), a 256×256 matrix, and 1.4 times oversampling in the section partitions axis; the total imaging time was 3 minutes 35 seconds.

The axial MT 3-D gradient-echo technique was performed with the same 3-D gradient-echo sequence, with exactly the same imaging parameters and measurement time. The MT pulse was 10 milliseconds in duration with a 200-Hz bandwidth and the pulse shape defined mathematically as $(1 - \cos x)$ from 0 to 2π . The transverse magnetization was RF-spoiled after application of the MT pulse and at the end of every TR (immediately before application of the MT pulse). The peak amplitude was 700 Hz, giving a root mean squared amplitude of 270 Hz. The specific absorption rate was approximately 4.0 W/kg. The frequency offset of the MT pulse was 1000 Hz off-resonance. Twenty-five milliseconds the minimum TR attainable with the 10-millisecond MT pulse and extra spoiling; the minimum TR of the base sequence was 12 milliseconds.

The axial T1-weighted spin-echo sequence was performed with parameters of 699/16/1, 24 5-mm-thick sections, a 25-cm FOV, a 256×256 matrix, a phase sampling ratio of 1.2 (the phase-encoding steps and phase-encoding axis FOV were both scaled by this factor, such that resolution was unchanged), with a total imaging time of 3 minutes 35 seconds. The T1-weighted spin-echo sequence did not have gradient motion compensation, which prolonged the TE to 20 milliseconds and increased the minimum TR per section, so that the desired brain coverage could not be obtained in the 3.5-minute imaging time.

The patients were injected with contrast material (Omniscan, Nycomed, Princeton, NJ), then a 3.5-minute coronal T1-weighted spin-echo examination (which was part of the clinical protocol but not used in the analysis) was begun. The T1-weighted gradient-echo sequence was performed first, followed by the MT 3-D gradient-echo sequence and the T1-weighted spin-echo sequence; all images were obtained within 4 to 16 minutes after the injection of contrast material. Afterward, any additional sequences required for clinical evaluation were performed. The doses of contrast agent ranged from 0.05 to 0.1 mmol/kg; patients with metastatic disease or primary brain

tumors received 0.1 mmol/kg, and those with acoustic schwannoma received 0.05 mmol/kg.

Data Analysis

Lesion Contrast.—Images were processed on an independent basis using region-of-interest (ROI) analysis. The 3-D gradient-echo, the MT 3-D gradient-echo, and the T1-weighted spin-echo images were evaluated in identical fashion. Sixty-two enhancing lesions that were present on all three sets of images were selected; diameters ranged from 8 mm to 8 cm. Visual inspection and profile plots were used to locate the regions of peak signal intensity of the enhancing lesions. The mean signal intensity values of operator-defined ROIs (circular or irregular, minimum of 10 pixels) were obtained as measurements of mean lesion signal intensity. The signal intensity of normal (disease- and edema-free) white matter from the centrum semiovale was used as the value for background brain signal intensity. The standard deviation of the signal of background air, obtained from a 64-pixel circular ROI, was used as the value of image noise. All values were normalized by a factor that took into account the receiver attenuation and image scale factors.

The C/N ratio was defined as the algebraic difference between the normalized signal intensities of the lesion and background white matter divided by the image noise ($C/N = [SI_{\text{lesion}} - SI_{\text{background}}]/\text{noise}$), where SI is signal intensity. The L/B ratio was defined as the normalized signal intensities of the lesion divided by that of background white matter ($L/B = SI_{\text{lesion}}/SI_{\text{background}}$). The MT ratio (MTR) of white matter was determined as follows: $MTR = (SI_{\text{no MT}} - SI_{\text{MT}})/SI_{\text{no MT}}$. The normalized signal intensity values of lesions, background white matter, and noise, and the respective C/N and L/B values ($n = 62$), were collated in a database of a commercial statistical analysis and graphics program (StatMost 2.5 for Windows, DataMost Corp, Salt Lake City, Utah). Statistical analysis of mean values was performed using a paired two-tailed Student's t test, with $P < .01$ indicating statistical significance.

Lesion Count.—Twenty-four of the 45 patients had intracranial metastatic disease from lung or breast carcinoma. These metastatic lesions were counted on the T1-weighted spin-echo, the 3-D gradient-echo, and the MT 3-D gradient-echo images. Film copies of the images from each of these sequences were prepared for each patient's examination, using a coded numerical identifier. Metastatic lesions were defined as discrete, intraaxial regions of increased signal intensity relative to background brain parenchyma that were determined not to be vascular or choroidal in nature and not to be one of the normally enhancing circumventricular organs. Lesions were circled and counted on all 24 of the 3-D gradient-echo examinations, then on the 24 MT 3-D gradient-echo examinations, and finally on the 24 T1-weighted spin-echo examinations, such that if there was any learned pattern of lesion recognition, it favored the T1-weighted spin-echo examinations. The numerical coding was then broken, and a data base was formulated with each patient's lesion count for the three different sequences. Each patient's examinations were then reviewed in aggregate, with any accompanying additional images from the patient's examination (ie, T2-weighted images and contrast-enhanced images in other planes) to determine the patient's true lesion burden. Lesion counts were compared by statistical analysis using paired two-tailed t tests.

Results

Lesion Contrast

The 3-D gradient-echo technique resulted in a mean C/N of 16.7 ± 4.7 and a mean L/B of 1.3 ± 0.1 . With the application of MT, the 3-D gradient-echo images showed a statistically significant decrease in

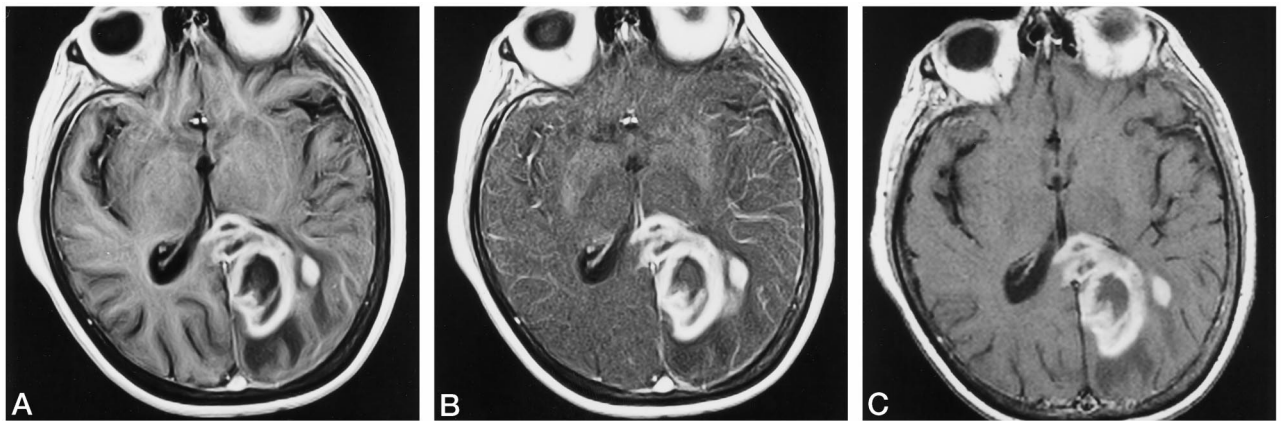


FIG 1. Glioblastoma multiforme in the left occipital region as seen on a T1-weighted 3-D gradient-echo image (25/4.4/1) (A), an MT 3-D gradient-echo image (699/16/1) (B), and a T1-weighted spin-echo image (699/16/1) (C). The contrast between the enhancing lesion and normal white matter background is greatest on the MT 3-D gradient-echo technique (B). Note that the vasogenic edema surrounding the tumor is most prominent on the 3-D gradient-echo image (A). With the application of MT (B), the vasogenic edema and background white matter are nearly isointense, but both are at a reduced signal intensity as compared with A.

the signal intensity of background white matter, from 31.5 ± 1.3 to 14.1 ± 0.6 ($P < .001$), yielding an MTR for white matter of 55% with this technique. There also was a slight but statistically significant decrease in the signal intensity of enhancing lesions with the application of MT, from 39.7 ± 1.9 to 36.3 ± 2.3 ($P < .01$), representing an MTR of 8.6% for the enhancing lesions. With the use of MT, C/N on the 3-D gradient-echo images improved 2.7 times, from 16.7 ± 4.7 to 46.0 ± 4.6 ($P < .001$), and L/B on the 3-D gradient-echo images improved 2.0 times, from 1.3 ± 0.1 to 2.6 ± 0.2 ($P < .001$). The T1-weighted spin-echo images had a mean C/N of 25.9 ± 5.3 and a mean L/B of 1.6 ± 0.1 . The C/N and L/B values on the T1-weighted spin-echo images were significantly greater than on the 3-D gradient-echo images, but less than on the MT 3-D gradient-echo images (all P values $< .01$).

A secondary image contrast feature observed was that vasogenic edema associated with mass lesions was seen consistently better on the 3-D gradient-echo images, with the T1-weighted spin-echo images next, and the MT 3-D gradient-echo images furnishing the lowest detection of edema. On T1-weighted sequences, vasogenic edema was of decreased signal intensity relative to normal white matter; edematous white matter also had a mildly reduced MTR relative to normal white matter. The signal intensity of both edematous and normal white matter was reduced by the MT pulse (the normal white matter to a greater extent), such that they had become essentially isointense. Ordinarily, the detection of vasogenic edema is not a critical element of contrast-enhanced T1-weighted imaging, as this is a task best performed with T2-weighted imaging, but the relationship between the edema and the margins of the enhancing tumor sometimes is of diagnostic importance. Figure 1 is of a patient with a glioblastoma multiforme, and illustrates both the enhancing lesion contrast and the detection of edema among the three imaging techniques.

Metastatic Lesion Count

The T1-weighted spin-echo images disclosed a total of 143 lesions (mean, six per patient), the 3-D gradient-echo images had a total of 122 lesions (mean, five per patient), and the MT 3-D gradient-echo images had a total of 179 lesions (mean, seven per patient). The paired two-tailed t test analysis of the three sequences revealed that the MT 3-D gradient-echo images had a significantly greater lesion count than did the T1-weighted spin-echo or 3-D gradient-echo images ($P < .001$ for both comparisons), and the T1-weighted spin-echo images showed significantly more lesions than did the 3-D gradient-echo images ($P < .01$). On review and cross correlation of individual metastatic lesions, using the detection criteria outlined previously, all the lesions enumerated prospectively on the MT 3-D gradient-echo images were considered actual metastases. Figure 2 shows the difference in detection of small metastatic lesions for the three techniques. In general, the lesions detected with the MT 3-D gradient-echo technique that were not seen on T1-weighted spin-echo or 3-D gradient-echo images were less than 6 mm in size, and, in fact, were faintly enhancing, but only to the point that they had become essentially isointense with background brain. Detection of these additional lesions did not have a direct impact on treatment in any of the patients.

A second cause of the decreased lesion count on the T1-weighted spin-echo images as compared with the MT 3-D gradient-echo images was pulsatile flow artifacts from the major arteries and dural sinuses, because the T1-weighted spin-echo sequences did not have flow compensation. Eight of the 24 patients had metastatic lesions that were masked on the T1-weighted spin-echo images by pulsatile flow artifacts. These were most often small, posterior fossa lesions that were obscured by ghosting artifacts arising from the transverse and sigmoid sinuses, as seen in Figure 3. In 38 of the 45 patients, notable ghosting artifacts on the T1-weighted spin-echo images needed to be

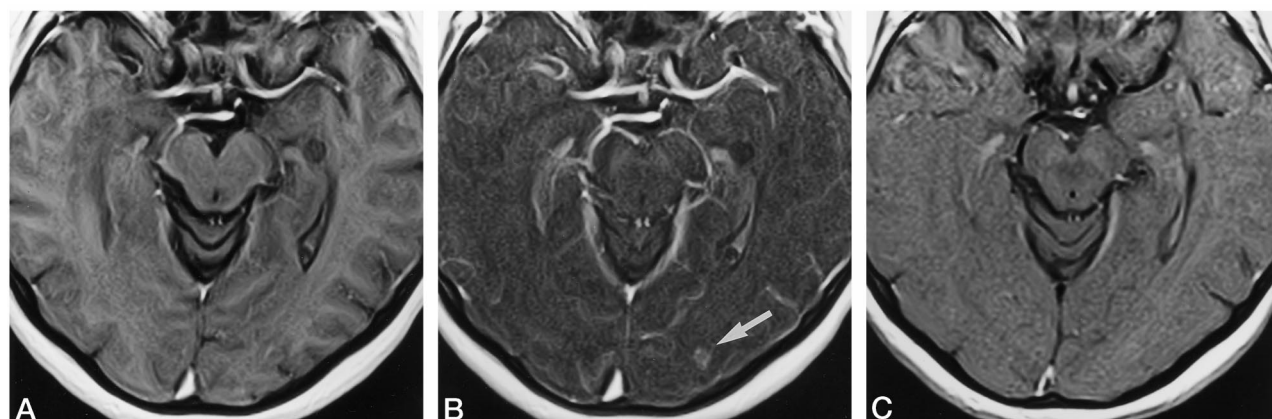


FIG 2. Metastatic breast carcinoma as depicted on a T1-weighted 3-D gradient-echo image (25/4.4/1) (A), an MT 3-D gradient-echo image (25/4.4/1) (B), and a T1-weighted spin-echo image (699/16/1) (C). A 3- to 4-mm metastatic lesion in the left occipital lobe (arrow, B) was correctly diagnosed only on the MT 3-D gradient-echo image. In retrospect, slight vasogenic edema and faint ring enhancement is seen on the 3-D gradient-echo image (A); the lesion is essentially imperceptible on the T1-weighted spin-echo image (C). An incidental, small ependymal cyst is seen at the margin of the temporal horn of the left lateral ventricle, which had been present on examinations prior to the development of metastases to the CNS.

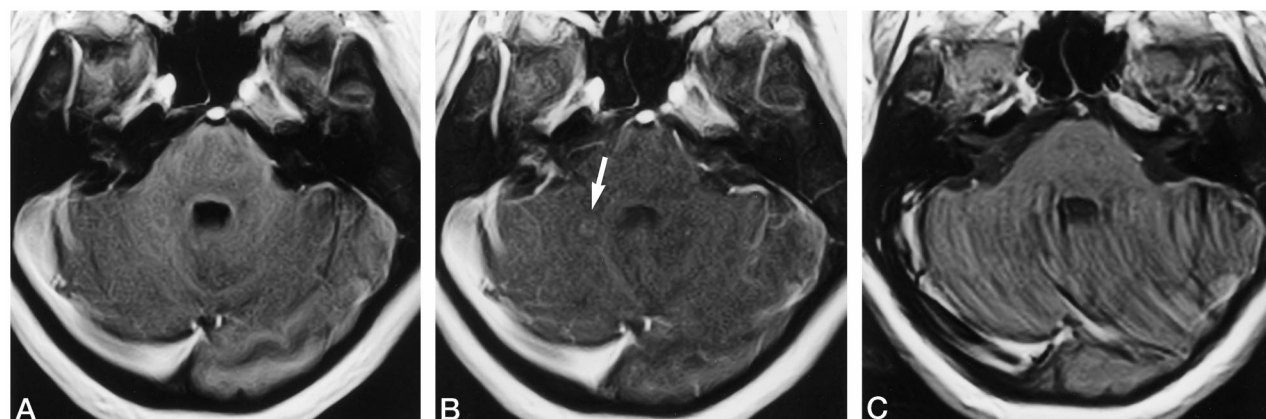


FIG 3. Metastatic lung carcinoma as seen on a T1-weighted 3-D gradient-echo image (25/4.4/1) (A), an MT 3-D gradient-echo image (25/4.4/1) (B), and a T1-weighted spin-echo image (699/16/1) (C). A 3-mm metastatic lesion is seen in the middle cerebellar peduncle on the 3-D gradient-echo and MT gradient-echo images (arrow, B). This lesion is completely lost in pulsatile ghosting artifacts from the transverse sinus on the T1-weighted spin-echo image (C).

detected, correctly diagnosed as artifactual, and ignored.

Discussion

We have demonstrated that MT can be successfully applied to short-TR, 3-D, RF-spoiled, T1-weighted gradient-echo imaging, resulting in significant improvement in the C/N and L/B ratios of enhancing lesions and in the metastatic lesion count as compared with conventional 3-D gradient-echo and T1-weighted spin-echo imaging. Integral to the performance of the MT 3-D gradient-echo sequence is the use of a relatively shorter MT pulse duration than has been used in other investigations, which allows a shorter-TR sequence. The concept of effective MT power in the context of the saturation duty cycle has been addressed by several investigators (11–13). The 10-millisecond MT pulse in the 25-millisecond TR sequence represents a relatively high MT pulse duty cycle (40%), and the available peak amplitude range

of the RF amplifier allows access to very high effective MT powers. With the MT 3-D gradient-echo sequence used in patient examinations, the maximum 4.0 W/kg specific absorption rate is a practical limitation to the amount of MT power one can apply. This application yields an MTR for normal white matter of approximately 55% in a strongly T1-weighted 3-D gradient-echo sequence.

Use of the 3-D gradient-echo technique solves the section coverage versus TR limitation that has been encountered in MT applications with T1-weighted spin-echo imaging. This limitation has caused investigators to obtain full brain coverage by either obtaining two packs of nine to 10 sections each in a sequence with TR of 500 to 600 (1) or prolonging the TR to nearly 1 second, pushing the limits of what would be considered “good” T1 weighting (4, 8). In this investigation, we thought it important to perform the MT imaging at a resolution and section coverage attainable by both spin-echo and 3-D gradient-echo techniques in relatively short overall imaging times.

This allowed all three sequences to be obtained in the 4- to 16-minute postcontrast window, the period during which previous investigators (20–24) have shown that lesion contrast reaches a plateau, with less than 10% variation. It is possible that the temporal enhancement kinetics of this study may have contributed in a minor positive fashion to the improvement in lesion contrast between the 3-D gradient-echo and MT 3-D gradient-echo sequences. We currently use the MT 3-D gradient-echo sequences clinically in a higher resolution mode, with 48 3-mm-thick sections obtained in a 20-cm FOV in under 5 minutes' imaging time.

We calculated two parameters of lesion contrast: an absolute measurement of contrast, C/N, and a relative measurement of contrast, L/B. This was done to facilitate comparison of the results with other studies in the literature, especially those in which T1-weighted spin-echo imaging with MT was used. Of the many studies documenting improved lesion contrast on contrast-enhanced T1-weighted spin-echo MT images, two included substantial quantitative data from patient examinations at high field strength that can be used for comparison with the MT 3-D gradient-echo technique. Finelli et al (4), using pulsed off-resonance MT techniques, and Mehta et al (8), using binomial on-resonance MT techniques, reported similar results in comparisons of lesion C/N on conventional T1-weighted spin-echo images versus that on T1-weighted spin-echo images with MT, showing a near doubling in C/N of enhancing brain lesions on the MT images. The C/N values reported in those studies were greater than those found in our study for the MT 3-D gradient-echo technique; however, a different MT pulse, sequence parameters, and longer imaging times were used. The corresponding relative contrast, calculated as L/B, reported by Finelli et al (4) was approximately 2.6, and that of Mehta et al (8) was approximately 2.1; thus, the L/B of approximately 2.6 we found with the MT 3-D gradient-echo technique represents a relative lesion contrast comparable to that achieved with MT T1-weighted spin-echo techniques. We also note that the mean L/B of the MT 3-D gradient-echo technique is in the range of that found in prior studies of conventional T1-weighted spin-echo techniques with triple-dose contrast agent (20–24).

The 3-D gradient-echo MT sequence used in this experiment produced a substantially greater MT effect than that exhibited in previous studies using spin-echo techniques (1–9), fundamentally because of a higher effective MT power. The MT pulse parameters that produce the greatest L/B for T1-weighted 3-D gradient-echo images are high effective MT power and narrow MT pulse-frequency offset (25); these are the same general rules that apply to T1-weighted spin-echo MT imaging. Ulmer et al (9) showed that one could take advantage of indirect (MT) saturation, direct saturation, and spin-locking effects to augment the L/B on T1-weighted spin-echo MT sequences by using small MT pulse-frequency offsets. The section-select flip angle of the 3-D RF-spoiled gradient-echo

sequence has a major influence on the T1 weighting of the sequence and therefore on the L/B contrast (26). Phantom studies using the MT 3-D gradient-echo sequence have suggested intralesional gadolinium concentration-dependent relationships between the section-select flip angle and the peak enhancing lesion contrast (25); however, a significant improvement in lesion contrast over that on non-MT 3-D gradient-echo sequences is observed over a broad range of flip angles (3° to 30°), which encompasses the usual range of flip angles used for T1-weighted applications of these short-TR gradient-echo sequences.

In conclusion, we have developed a T1-weighted MT 3-D gradient-echo technique that has enhancing lesion contrast comparable to that of T1-weighted MT spin-echo imaging but with the sampling and image coverage attributes of high-resolution 3-D RF-spoiled gradient-echo imaging. The detectability of enhancing lesions depends fundamentally on C/N and resolution, and the MT 3-D gradient-echo technique has the ability to address both issues well.

References

1. Elster AD, King JC, Mathews VP, Hamilton CA. **Cranial tissues: appearance at gadolinium-enhanced and nonenhanced MR imaging with magnetization transfer contrast.** *Radiology* 1994;190:541–546
2. Tanttu JI, Sepponen RE, Lipton MJ, Kuusela T. **Synergistic enhancement of MRI with Gd-DTPA and magnetization transfer.** *J Comput Assist Tomogr* 1992;16:19–24
3. Kurki TJ, Niemi PT, Lundbom N. **Gadolinium-enhanced magnetization transfer contrast imaging of intracranial tumors.** *J Magn Reson Imaging* 1992;2:401–406
4. Finelli DA, Hurst GC, Gullapalli RP, Bellon EM. **Improved contrast of enhancing brain lesions on post-gadolinium, T1-weighted spin-echo images with use of magnetization transfer.** *Radiology* 1994;190:553–559
5. Mathews VP, King JC, Elster AD, Hamilton CA. **Cerebral infarction: effects of dose and magnetization transfer at gadolinium-enhanced MR imaging.** *Radiology* 1994;190:547–552
6. Mathews VP, Elster AD, King JC, et al. **Combined effects of magnetization transfer and gadolinium in cranial MR imaging and MR angiography.** *AJR Am J Roentgenol* 1995;164:169–172
7. Runge VM, Wells JW, Kirsch JE. **Magnetization transfer and high dose contrast in early brain infection on magnetic resonance.** *Invest Radiol* 1995;30:135–143
8. Mehta RC, Pike GB, Haros SP, Enzmann DR. **Central nervous system tumor, infection, and infarction: detection with gadolinium-enhanced magnetization transfer imaging.** *Radiology* 1995;195:41–46
9. Ulmer JL, Mathews VP, Hamilton CA, Elster AD, Moran PR. **Magnetization transfer or spin-lock? An investigation of off-resonance saturation pulse imaging with varying frequency offsets.** *AJNR Am J Neuroradiol* 1996;17:805–819
10. Moran PR, Hamilton CA. **Near-resonance spin-lock contrast.** *Magn Reson Imaging* 1995;13:837–846
11. McGowan JC, Schnall MD, Leigh JS. **Magnetization transfer imaging with pulsed off-resonance saturation: variation in contrast with saturation duty cycle.** *J Magn Reson Imaging* 1994;4:79–82
12. Hua J, Hurst GC. **Analysis of on- and off-resonance magnetization transfer techniques.** *J Magn Reson Imaging* 1995;5:113–120
13. Finelli DA, Hurst GC, Amantia P, Gullapalli RP, Apicella A. **Cerebral white matter: technical development and clinical applications of effective MT power concepts for high-power, thin-section, quantitative MT examinations.** *Radiology* 1996;199:219–226
14. Mirowitz, SA. **Intracranial lesion enhancement with gadolinium: T1-weighted spin echo vs. three-dimensional Fourier transform gradient echo MR imaging.** *Radiology* 1992;185:529–534
15. Ross JS, Masaryk TJ, Modic MT. **Three dimensional FLASH imaging: applications with gadolinium-DTPA.** *J Comput Assist Tomogr* 1989;13:547–552
16. Chappell PM, Pelc NJ, Foo TKF, Glover GH, Haros SP, Enzmann

- DR. Comparison of lesion enhancement on spin-echo and gradient-echo images. *AJNR Am J Neuroradiol* 1994;15:37-44
17. Rand S, Maravilla KR, Schmiedl U. Lesion enhancement in radio-frequency spoiled gradient echo imaging: theory, experimental evaluation, and clinical implications. *AJNR Am J Neuroradiol* 1994;15:27-35
 18. Mugler JP III, Brookeman JR. Theoretical analysis of gadopentetate dimeglumine enhancement in T1-weighted imaging of the brain: comparison of 2D spin echo and three-dimensional gradient-echo sequences. *J Magn Reson Imaging* 1993;3:761-769
 19. Li D, Haacke EM, Tarr RW, Venkatesan R, Lin W, Wielopolski P. Magnetic resonance imaging of the brain with gadopentetate dimeglumine-DTPA: comparison of T1-weighted spin-echo and 3D gradient-echo sequences. *J Magn Reson Imaging* 1996;6:415-424
 20. Yuh WTC, Engelken JD, Muhonen MG, Mayr NA, Fisher DJ, Ehrhardt JC. Experience with high-dose gadolinium MR imaging in the evaluation of brain metastases. *AJNR Am J Neuroradiol* 1992;13:335-345
 21. Haustein J, Laniado M, Niendorf HP, et al. Administration of gadopentetate dimeglumine in MR imaging of intracranial tumors: dosage and field strength. *AJNR Am J Neuroradiol* 1992;13:1199-1206
 22. Yuh WTC, Nguyen HD, Tali ET, et al. Delineation of gliomas with various doses of MR contrast material. *AJNR Am J Neuroradiol* 1994;15:983-989
 23. Haustein J, Laniado M, Niendorf HP, et al. Triple dose versus standard dose gadopentetate dimeglumine: randomized study in 199 patients. *Radiology* 1993;186:855-860
 24. Yuh WTC, Tali ET, Nguyen HD, et al. Effect of contrast dose, imaging time, and lesion size in the MR detection of intracerebral metastases. *AJNR Am J Neuroradiol* 1995;16:373-380
 25. Finelli DA. Analysis of magnetization transfer effects on T1-weighted 3D GRE images using a phantom simulating enhancing lesions. *AJNR Am J Neuroradiol* 1997;18:147-159
 26. Pelc NJ. Optimization of flip angle for T1 dependent contrast in MRI. *Magn Reson Med* 1993;29:695-699